JACS
JOURNAL OF THE AMERICAN CHEMICAL SOCIETY

Communication

pubs.acs.org/JACS

Highly Selective Solar-Driven Methanol from CO_2 by a Photocatalyst/Biocatalyst Integrated System

Rajesh K. Yadav, Gyu Hwan Oh, No-Joong Park, Abhishek Kumar, Ki-jeong Kong, and Jin-Ook Baeg*

Division of Green Chemistry and Engineering Research, Korea Research Institute of Chemical Technology (KRICT), 100 Jang-dong, Yuseong, Daejeon 305 600, Republic of Korea

Supporting Information

ABSTRACT: The successful development of a photocatalyst/biocatalyst integrated system that carries out selective methanol production from CO_2 is reported herein. The fine-tuned system was derived from a judicious combination of graphene-based visible light active photocatalyst (CCG-IP) and sequentially coupled enzymes. The covalent attachment of isatin-porphyrin (IP) chromophore to chemically converted graphene (CCG) afforded newly developed CCG-IP photocatalyst for this research endeavor. The current work represents a new benchmark for carrying out highly selective methanol formation from CO_2 in an environmentally benign manner.

The ever increasing fossil fuel demand and a concomitant rise in atmospheric CO_2 levels demands concerted carbon management. Therefore, conversion of CO_2 into fuels and chemicals has been envisaged.[1] In this context, development of systems for the fixation of CO_2 into methanol is particularly interesting. Consequently, a number of studies on multi-electron reduction of CO_2 to methanol have being carried out so far. For instance, chemical reduction of CO_2 to methanol by organometallic and inorganic catalysts has been reported. Despite the use of hydrogen gas or hydride ion along with high temperature and/or high pressure, they afford methanol in poor selectivity.[1−7] The electrocatalytic reduction of CO_2 leads to methanol formation in higher selectivity. However, it requires a continuous supply of electricity which is primarily obtained from fossil fuels and hence environmentally unfavorable.[1,8]

Solar light is the ideal energy source from a sustainable perspective. Therefore, the use of photocatalysts for solar-driven methanol from CO_2 is a very attractive approach. Hence a variety of inorganic semiconductors and metal complexes as photocatalysts or photoelectrocatalysts have been evaluated. However, most of them provide low yields with poor product selectivity along with the requirement of UV light for photoreduction.[7,9−14]

It is quite evident from literature that obtaining methanol from CO_2 in high selectivity continues to be a major challenge. The biocatalysts or enzymes are known to carry out highly selective transformations at ambient conditions. Therefore, the reduction of CO_2 to methanol using enzymes has also been explored.[15−17] However, enzymes require a stoichiometric amount of expensive NADH cofactor to carry out biocatalysis. It is therefore necessary to develop economical methods for NADH cofactor regeneration. To achieve this goal, electrochemical regeneration of NADH has been developed over the last few decades.[18,19] Although intensively researched, it continues to suffer from serious drawbacks such as slow electron-transfer rate, low yields, and poor selectivity. These limitations can be overcome by a photocatalyst/biocatalyst integrated system wherein clean and abundantly available solar light is directly used by the photocatalyst for continuous NADH regeneration, which is utilized by the enzymes to produce solar fuel. Quite surprisingly, the potential of such an environmentally benign strategy to obtain methanol exclusively from CO_2 remains unexplored. We now herein report the development of a photocatalyst/biocatalyst integrated system to achieve this aim.[20] The system for this study was obtained by combining our newly developed graphene-based photocatalyst with sequentially coupled enzymes (formate dehydrogenase, formaldehyde dehydrogenase, and alcohol dehydrogenase) as depicted in Scheme 1. To the best of our knowledge, this is the first report on exclusive methanol formation from CO_2 directly by visible light-driven photocatalyst/biocatalyst integrated system.

A visible light photocatalyst with broad spectral absorption for efficient light harvesting and concomitant electron transfer is a prerequisite for this research work. One may therefore assume

Scheme 1. Schematic Illustration of the CCG-IP Photocatalyst/Biocatalyst Integrated System for Carrying out Methanol Formation From CO_2[a]

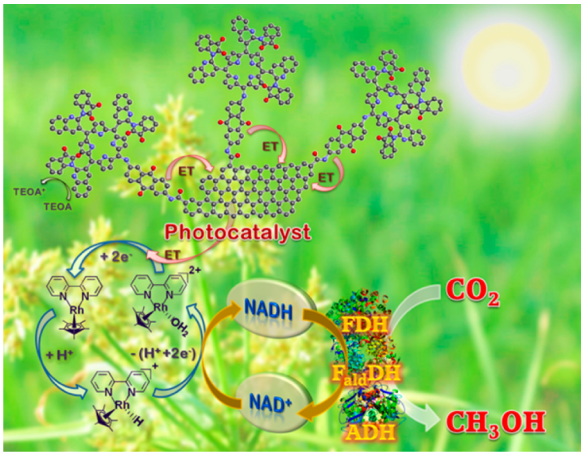

[a]FDH = formate dehydrogenase, $F_{ald}DH$ = formaldehyde dehydrogenase, ADH = alcohol dehydrogenase.

Received: September 18, 2014

   dx.doi.org/10.1021/ja509650r | J. Am. Chem. Soc. XXXX, XXX, XXX−XXX

that any visible light active photocatalyst might be suitable for the task. We recently reported a system for CO_2 reduction to formic acid utilizing visible light by developing chemically converted graphene coupled multi-anthraquinone-substituted porphyrin (CCGCMAQSP) photocatalyst.[21] Thus, CCGCMAQSP was initially evaluated for this research endeavor. However, it provided rather poor results (vide infra). For improved performance, two highly versatile chromophoric motifs, isatin and porphyrin, were combined together.[22] The trisubstitution of isatin onto porphyrin ring provided 1,1′,1″-((20-(2-((7-amino-9,10-dioxo-9,10-dihydroanthracen-2-yl)amino)quinolin-3-yl) porphyrin-5,10,15-triyl) tris (quinoline-3,2-diyl)) tris(indoline-2,3-dione) (hereinafter IP) as a suitable chromophore for our research work. The subsequent covalent attachment of IP chromophores with chemically converted graphene (CCG) led to the robust CCG-IP photocatalyst (Figure 1) which was

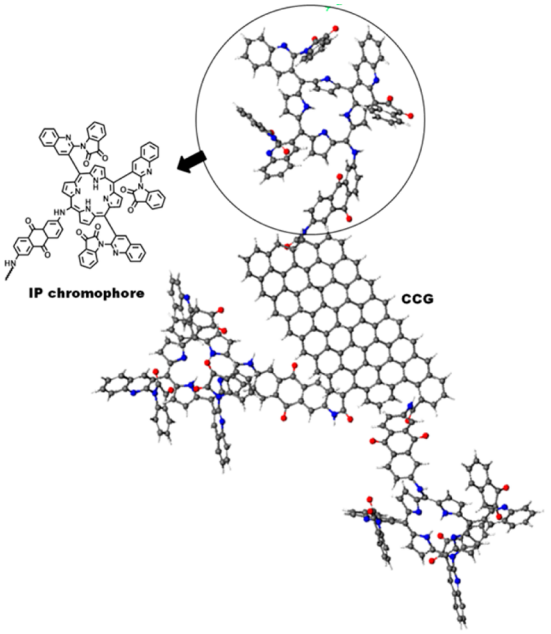

Figure 1. 3D structure of CCG-IP photocatalyst alongwith detailed chemical structure of IP chromophore.

characterized by various techniques such as atomic force microscopy, X-ray photoelectron spectroscopy, energy-dispersive X-ray spectroscopy, Fourier transform infrared spectroscopy, Raman spectroscopy, and thermogravimetric analysis. The details of all these analysis are provided in the Supporting Information (SI).

The absorption spectrum of CCG-IP (Figure S6, SI) exhibits a strong soret band at 480 nm. The IP chromophore also exhibits absorption band at similar wavelength albeit with lower absorption.[23] On the other hand, isatin and 2,6-diaminoanthraquinone (AAQ) exhibit much lower absorption in 400−500 nm range. These observations indicate that CCG-IP is capable of efficient visible light harvesting and thus provides photocatalytic energy for regeneration of enzymatically active 1,4-NADH in high efficiency, which is indispensable for methanol formation from CO_2.[24,25]

The role of photocatalyst in the integrated system is to harness visible light for carrying out continuous regeneration of 1,4-NADH. Therefore, to begin with, CCG-IP was examined for its visible light-driven 1,4-NADH photoregeneration ability. The system was initially allowed to equilibriate in dark for 30 min, followed by exposure to visible light (1 sun). As shown in Figure 2a, CCG-IP was successful in photoregeneration with constant

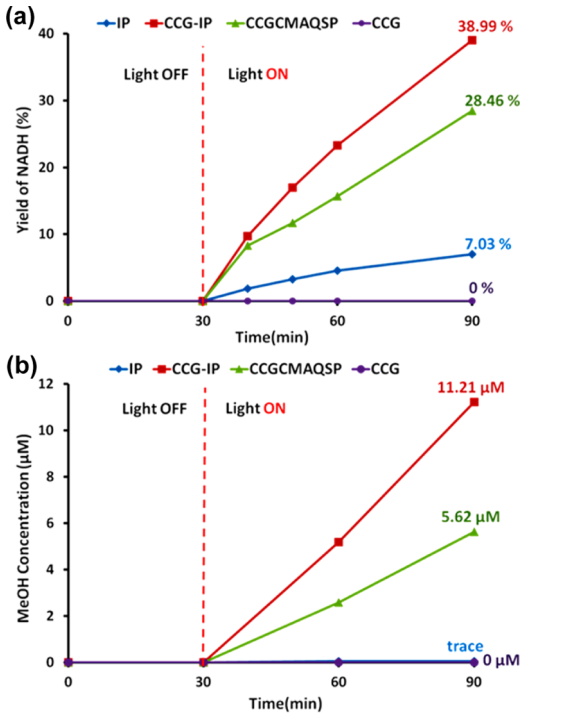

Figure 2. (a) Photocatalytic 1,4-NADH regeneration activity of CCG-IP, CCGCMAQSP, IP, and CCG photocatalyst [β-NAD^+ (1.24 μmol), rhodium complex $[Cp^*Rh(bpy)H_2O]^{2+}$ **Rh** (0.62 μmol), TEOA (1.24 mmol), and photocatalyst (0.5 mg) in 3.1 mL of sodium phosphate buffer (100 mM, pH 7.0)]. (b) Exclusive production of methanol from CO_2 (flow rate: 0.5 mL/min) under visible light by CCG-IP, CCGCMAQSP, IP, and CCG upon integration with enzymes [β-NAD^+ (1.24 μmol), **Rh** (0.62 μmol), TEOA (1.24 mmol), photocatalyst (0.5 mg), and 9 units of each enzyme (formate dehydrogenase, formaldehyde dehydrogenase, and alcohol dehydrogenase) in 3.1 mL of sodium phosphate buffer (100 mM, pH 7.0)].

NADH accumulation of 38.99% linearly over a period of the next 60 min. On the other hand, CCGCMAQSP photocatalyst and IP chromophore provided 28.46 and 7.03% of NADH regeneration in the same time frame, respectively. CCG failed to carry out any NADH regeneration. We then evaluated CCG-IP and CCGCMAQSP as photocatalyst of the integrated system for methanol formation from CO_2. Following the bubbling of CO_2 in dark for 30 min, methanol concentration of 11.21 μM was obtained on exposure to visible light over the next 60 min when CCG-IP was used as the photocatalyst (Figure 2b). On the other hand, only 5.62 μM of methanol concentration was obtained upon the use of CCGCMAQSP as photocatalyst. The experiment with IP chromophore provided trace amount of methanol which could not be quantified, while CCG failed to produce any methanol. From these experiments, the notably higher photocatalytic performance of CCG-IP in carrying out exclusive methanol production from CO_2 is clearly evident.

To rule out photocatalytic methanol formation by some carbon residues in the reaction mixture,[26] a control experiment in the absence of CO_2 was performed. However, no methanol formation was observed in this experiment. In a related manner, one control experiment without the CCG-IP photocatalyst (but with enzymes) and another one without visible light irradiation were performed. No methanol formation in these cases

dx.doi.org/10.1021/ja509650r | J. Am. Chem. Soc. XXXX, XXX, XXX−XXX

confirmed photocatalytic NADH regeneration by CCG-IP under visible light irradiation. A set of control experiments in the absence of **Rh** and/or NAD^+ also failed to produce any methanol. Overall the control experiments clearly point toward visible light-driven NADH regeneration and subsequent methanol formation from CO_2 by the photocatalyst/biocatalyst integrated system.

The stability and reusability of the photocatalyst were also examined. The photocatalyst was subjected to three cycles of NADH regeneration. In comparison to the first cycle wherein the photocatalyst carried out 38.99% (100%) of NADH regeneration, 36.81% (94.41%) was obtained in the third cycle (Figure S7, SI). This remarkably high photocatalytic activity indicates a stable and reusable photocatalyst.

To elucidate the photoinduced electron-transfer mechanism, electrochemical studies were performed. The reduction potential at cathodic peak current of **Rh** and CCG-IP was observed at around −0.72 V (Figure 3a) and −0.92 V (Figure S8, SI),

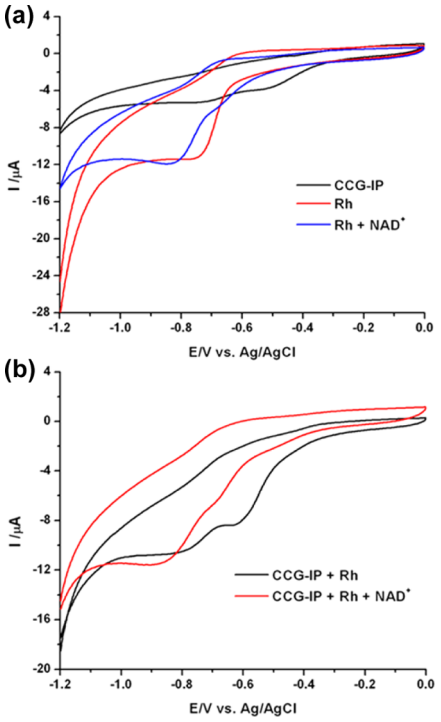

Figure 3. Cyclic voltammograms of (a) CCG-IP (10 μM), **Rh** (0.2 mM), and **Rh** with NAD^+ (0.4 mM) solutions. (b) Mixture of two components (**Rh** and CCG-IP) in the absence and presence of NAD^+ (0.4 mM). The potential was scanned at 100 mV s^{-1} using glassy carbon (working), silver-silver chloride (reference), and platinum (counter) electrodes in sodium phosphate buffer (100 mM, pH 7.0).

respectively. However, on mixing together the two components (**Rh** and CCG-IP) in solution, reduction was observed at −0.80 V. It is a cathodic shift of **Rh** reduction, or in other words, an anodic shift of CCG-IP reduction (Figure 4b) which indicates electron transfer from CCG-IP to **Rh**.[21] The CCG-IP-**Rh** system revealed an increase in reduction peak current with NAD^+, implying that the system consisting of CCG-IP and **Rh** catalyzes the reduction of NAD^+ to NADH (Figure 3b). As per literature, the catalytic effect of **Rh** results in strongly increased rate of **Rh** reduction in the presence of NAD^+.[21] From these observations, one may conclude that the transfer of electrons from TEOA to CCG-IP results in the electrical reduction of **Rh**. The vicinity and potential gradient between the light harvesting CCG-IP

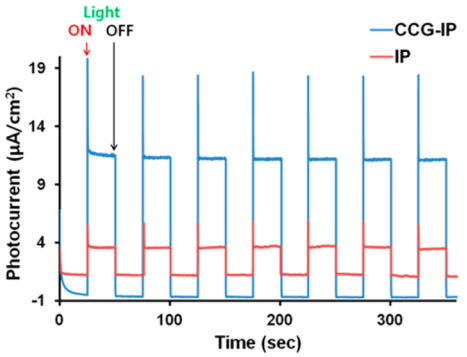

Figure 4. Photocurrent−time (I−T) profiles of FTO/IP and FTO/CCG-IP electrodes under simulated solar light (1 sun) illumination (three electrodes; scan rate 50 mV/s; input power: 100 mW/cm^2; and electrolyte: 0.1 M NaCl in water, bias potential: 0−0.1 V (vs Ag/AgCl)). The photo electrochemical test device was fabricated by drop casting the photocatalyst dispersed in DMF (0.01g/mL) onto fluorine-doped tin oxide (FTO)-coated glass.

photocatalyst and the electrocatalytic center **Rh** enables the electron transfer from former to latter. The electrically reduced **Rh** thus obtained is chemically protonated in aqueous media, followed by its catalytic regeneration of enzymatically active-1,4-NADH in high yield.

For a better understanding, transient photocurrent study was also carried out. A significantly higher photocurrent was observed with CCG-IP in comparison to IP electrode (Figure 4). The prompt photocurrent response of CCG-IP corresponded well with ON/OFF cycles of simulated sun light irradiation. It indicates electron transfer from IP to CCG upon irradiation leading to regeneration of enzymatically active 1,4-NADH and subsequent methanol formation.[21]

The origin of photocatalytic activity and activity enhancement of the graphene-based photocatalyst was also investigated theoretically by a series of first-principles calculations. The geometry optimizations and electronic properties of CCG and IP were carried out in the framework of the density functional theory (DFT) by using the B3LYP exchange−correlation potential[27,28] as implemented in DMol^3.[29] Double numerical polarized (DNP) basis set that includes all occupied atomic orbitals plus a second set of valence atomic orbitals plus polarized d-valence orbitals was employed. The theoretically obtained atomic geometries and the wave functions of HOMO (highest occupied molecular orbital) and LUMO (lowest unoccupied molecular orbital) are shown in Figure 5.

The incident light is absorbed at IP, where photoexcitation occurs, and the created electrons in LUMO move into CCG via stable amide bond. The electron-transfer efficiency could be

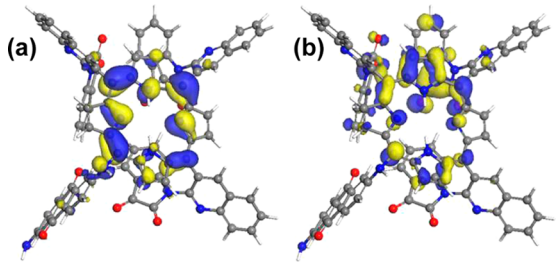

Figure 5. Visualization of the molecular orbitals of IP (a) HOMO and (b) LUMO as obtained from DFT calculations.

dx.doi.org/10.1021/ja509650r | J. Am. Chem. Soc. XXXX, XXX, XXX−XXX

estimated by the energy level alignment between the Fermi level of CCG and the LUMO of IP chromophore system. From our DFT calculation results, we confirmed that the energy levels of each segment are aligned for electrons to be able to transfer from IP finally to hydrogen reduction site via CCG. The Fermi level of graphene lies between HOMO−LUMO gap, about 0.97 eV lower than the LUMO level of IP. Thus, photoexcited electrons in LUMO of IP can be easily transferred into CCG by the use of this potential difference. By virtue of high potential difference, the transferred charge carriers in CCG are hot electrons which have sufficient energy to overcome the hydrogen reduction overpotential on the rhodium complex. As is well-known, graphene exhibits remarkably high electron mobility up to 200,000 $cm^2/V{\cdot}s$ at a carrier density of 10^{12} cm^{-2} at room temperature.[30] By virtue of the extraordinary high mobility of carriers in addition to the huge surface area, the transferred electrons can reach reduction sites far away, resulting in the enhancement of catalytic activity. Furthermore, the graphene also acts as an electron reservoir to transport multiple electrons. In most molecular systems, the energy cost of electron addition is very high because of large Coulomb repulsion between localized electrons. In graphene, the multi-electron addition or removal can be possible because of the delocalized nature of wave functions over the entire graphene surface (extending several μm).

In order to gain some insight into the electron transfer between CCG and IP moieties, time-resolved fluorescence study on CCG-IP was performed by time-correlated single photon counting control technique. From the decay time profiles, data of the photoexcited IP in CCG-IP (λ_{ex} = 480 nm) were curve-fitted using biexponential decay kinetics, from which lifetimes of 1.06 ns (10.58%) and 8.96 ns (89.42%) were deduced. On the other hand, lifetime of intact IP chromophore (λ_{ex} = 479 nm) was estimated to be 3.71 ns (100%). Thus, it is reasonable to assume a charge separation and charge recombination scenario in CCG-IP via IP* with rate constants of 1.9×10^8 and 0.7×10^8 s^{-1}, respectively.[31]

In summary, we have successfully demonstrated a photocatalyst/biocatalyst integrated system for highly selective methanol production from CO_2 directly. Our newly developed photocatalyst (CCG-IP) is capable of harvesting sufficient visible light for carrying out the multi-electron reduction of CO_2 to methanol at ambient conditions upon integration with the sequentially coupled enzymes. To the best of our knowledge, this is the first report on CO_2 fixation exclusively as methanol by a photocatalyst/biocatalyst integrated system. On the whole, our approach provides an appealing strategy for selective methanol production from CO_2 by the use of inexpensive and abundantly available solar energy.

■ ASSOCIATED CONTENT

Supporting Information

Synthesis details and characterization data for CCG-IP photocatalyst. This material is available free of charge via the Internet at http://pubs.acs.org.

■ AUTHOR INFORMATION

Corresponding Author

jobaeg@krict.re.kr

Notes

The authors declare no competing financial interest.

■ ACKNOWLEDGMENTS

This work was supported by the KRICT 2020 project program.

■ REFERENCES

(1) Kondratenko, E. V.; Mul, G.; Baltrusaitis, J.; Larrazábal, G. O.; Pérez-Ramírez, J. *Energy Environ. Sci.* **2013**, *6*, 3112.
(2) Riduan, S. N.; Zhang, Y.; Ying, J. Y. *Angew. Chem., Int. Ed.* **2009**, *48*, 3322.
(3) Ménard, G.; Stephan, D. W. *J. Am. Chem. Soc.* **2010**, *132*, 1796.
(4) Huff, C. A.; Sanford, M. S. *J. Am. Chem. Soc.* **2011**, *133*, 18122.
(5) Jessop, P. G.; Joó, F.; Tai, C.-C. *Coord. Chem. Rev.* **2004**, *248*, 2425.
(6) Wesselbaum, S.; vom Stein, T.; Klankermayer, J.; Leitner, W. *Angew. Chem., Int. Ed.* **2012**, *51*, 7499.
(7) Wang, W.; Wang, S.; Ma, X.; Gong, J. *Chem. Soc. Rev.* **2011**, *40*, 3703.
(8) Benson, E. E.; Kubiak, C. P.; Sathrum, A. J.; Smieja, J. M. *Chem. Soc. Rev.* **2009**, *38*, 89.
(9) (a) Tseng, I.-H.; Wu, J. C. S.; Chou, H.-Y. *J. Catal.* **2004**, *221*, 432. (b) Pathak, P.; Meziani, M. J.; Castillo, L.; Sun, Y.-P. *Green Chem.* **2005**, *7*, 667. (c) Wang, C.; Thompson, R. L.; Baltrus, J.; Matranga, C. *J. Phys. Chem. Lett.* **2010**, *1*, 48.
(10) Ahmed, N.; Shibata, Y.; Taniguchi, T.; Izumi, Y. *J. Catal.* **2011**, *279*, 123.
(11) Cao, L.; Sahu, S.; Anilkumar, P.; Bunker, C. E.; Xu, J.; Fernando, K. A. S.; Wang, P.; Guliants, E. A.; Tackett, K. N., II; Sun, Y.-P. *J. Am. Chem. Soc.* **2011**, *133*, 4754.
(12) Habisreutinger, S. N.; Schmidt-Mende, L.; Stolarczyk, J. K. *Angew. Chem., Int. Ed.* **2013**, *52*, 7372.
(13) Boston, D. J.; Xu, C.; Armstrong, D. W.; MacDonnell, F. M. *J. Am. Chem. Soc.* **2013**, *135*, 16252.
(14) Rajeshwar, K.; de Tacconi, N. R.; Ghadimkhani, G.; Chanmanee, W.; Janáky, C. *ChemPhysChem* **2013**, *14*, 2251.
(15) Obert, R.; Dave, B. C. *J. Am. Chem. Soc.* **1999**, *121*, 12192.
(16) Xu, S.-w.; Lu, Y.; Li, J.; Jiang, Z.-y.; Wu, H. *Ind. Eng. Chem. Res.* **2006**, *45*, 4567.
(17) Kuwabata, S.; Tsuda, R.; Yoneyama, H. *J. Am. Chem. Soc.* **1994**, *116*, 5431.
(18) Hollmann, F.; Schmid, A.; Steckhan, E. *Angew. Chem., Int. Ed.* **2001**, *40*, 169.
(19) Wu, H.; Tian, C.; Song, X.; Liu, C.; Yang, D.; Jiang, Z. *Green Chem.* **2013**, *15*, 1773 and references cited therein..
(20) There is a report on photochemical/biocatalytic methanol synthesis from formaldehyde by the photoreduction of toxic methyl viologen. Amao, Y.; Watanabe, T. *Appl. Catal., B* **2009**, *86*, 109.
(21) Yadav, R. K.; Baeg, J.-O.; Oh, G. H.; Park, N.-J.; Kong, K.-j.; Kim, J.; Hwang, D. W.; Biswas, S. K. *J. Am. Chem. Soc.* **2012**, *134*, 11455.
(22) Sumpter, W. C. *Chem. Rev.* **1944**, *35*, 393.
(23) Niyogi, S.; Bekyarova, E.; Itkis, M. E.; McWilliams, J. L.; Hamon, M. A.; Haddon, R. C. *J. Am. Chem. Soc.* **2006**, *128*, 7720.
(24) Xu, Y.; Liu, Z.; Zhang, X.; Wang, Y.; Tian, J.; Huang, Y.; Ma, Y.; Chen, Y. *Adv. Mater.* **2009**, *21*, 1275.
(25) Guo, Z.; Du, F.; Ren, D.; Chen, Y.; Zheng, J.; Liu, Z.; Tian, J. *J. Mater. Chem.* **2006**, *16*, 3021.
(26) Yang, C.-C.; Vernimmen, J.; Meynen, V.; Cool, P.; Mul, G. *J. Catal.* **2011**, *284*, 1.
(27) Becke, A. D. *Phys. Rev. A* **1988**, *38*, 3098.
(28) Lee, C.; Yang, W.; Parr, R. G. *Phys. Rev. B* **1988**, *27*, 785.
(29) (a) Delley, B. *J. Chem. Phys.* **1990**, *92*, 508. (b) Delley, B. *J. Chem. Phys.* **2000**, *113*, 7756.
(30) Chen, J.; Jang, C.; Xiao, S.; Ishigami, M.; Fuhrer, M. S. *Nat. Nanotechnol.* **2008**, *3*, 206.
(31) Kodis, G.; Terazono, Y.; Liddell, P. A.; Andréasson, J.; Garg, V.; Hambourger, M.; Moore, T. A.; Moore, A. L.; Gust, D. *J. Am. Chem. Soc.* **2006**, *128*, 1818.